On the stability of colliding flows: radiative shocks, thin shells, and supersonic turbulence

Rolf Walder
Institute of Astronomy, ETH Zürich (walder@astro.phys.ethz.ch)

Doris Folini
Seminar of Applied Mathematics, ETH Zürich (folini@astro.phys.ethz.ch)

Abstract. High-resolution numerical simulations reveal the turbulent character of the interaction zone of colliding, radiative, hypersonic flows.

As the shocked gas cools radiatively, the cooled matter is squeezed into thin, high density shells. The remaining kinetic energy causes supersonic turbulence within these shells, before it is finally dissipated by internal shocks and vortex cascades. The density is far from homogeneous. High density filaments and large voids coexist. Its mean value is significantly below the stationary value. Similarly, areas with supersonic velocities are found next to subsonic regions. The mean velocity is slightly below or above the sound speed. While quasi uniform flow motions are observed on smaller scales the large scale velocity distribution is isotropic. Part of the turbulent shell is occupied by relatively uniform flow-patches, resembling coherent structures.

Astronomical implications of the turbulent interaction zone are multifarious. It probably drives the X-ray variability in colliding wind binaries as well as the surprising dust formation on orbital scales in some WR-binaries. It lets us understand the knotty appearance of wind-driven structures as planetary and WR-ring nebulae, symbiotics, supernova remnants, galactic supperbubbles. Also, WR and other radiatively driven, clumpy winds, advection dominated accretion, cooling flows and molecular cloud dynamics in star-forming regions may carry its stamp[1].

Keywords: hydrodynamics, colliding flows, turbulence, structure formation, stability, radiative cooling, shocks

1. Introduction

Colliding radiative hypersonic flows are a decisive ingredient of many astrophysical objects: the helio-pause, wind-driven structures, colliding wind binaries, and jets on all scales are obvious examples. But the phenomenon is also present in radiatively driven winds, in accretion- and cooling flows, and in the dynamics of star-forming molecular clouds. Even though certainly many more physical processes are essential in these different examples (magnetic fields, gravitation, radiation, particle acceleration), colliding hypersonic flows leave a common trace: thin shells of compressed, cold gas form within the hot, shocked flow,

[1] Colored pictures, mpeg-videos as well as papers by the authors can be taken from http://www.astro.phys.ethz.ch/staff/walder/ and .../folini/ .

whenever energy can escape from the collision zone (most easily by optically thin radiative emission, but also by heat transfer due to thermal electrons and ions, by photon diffusion or by accelerated particles).

Numerical simulations immediately revealed that colliding flow interaction zones carrying such shells are unstable. From the extensive literature we only refer to Hunter et al. (1986), who investigate star formation, and to Stevens et al. (1992), who study colliding wind binaries. The interaction zones are subject to a variety of instabilities. Classical interface instabilities, like Rayleigh-Taylor, behave differently in the context of thin shells than in 'open' areas. There are also a number of special 'thin shell' instabilities. Here we only mention the non-linear thin shell instability (NTSI), analytically analyzed for planar symmetry by Vishniac (1994) and numerically by Blondin and Marks (1996). Results for some of these thin shell instabilities have been verified in the laboratory, e.g. the decelerating instability (Grun et al., 1991). The cooling process of the shocked flow itself is unstable under many circumstances. Further references can be taken from recent reviews by Draine and McKee (1993) and by Walder and Folini (1998a).

Here we present some preliminary results focusing on the quasi-stationary state of the driven supersonic turbulence developing in shock-bounded shells. Under what circumstances such shells become unstable, what mechanisms are driving the turbulence, and other important questions we postpone, due to lack of space, to a subsequent paper (Folini and Walder, 2000a). We only note that the NTSI is neither the only instability present nor is it the only mechanism capable of exciting the turbulence. A joint action of different instabilities is also possible. And while non-infinitesimal disturbances of the shell seem essential, they may be provided 'naturally' by other – linear – instabilities. Finally, we remark that the temperature of the shell probably affects the growth scale of unstable modes and – qualitatively – some characteristics of the turbulence. This assumption is supported by the report of Myasnikov et al. (1998) on the temperature dependence of unstable modes in colliding wind binaries. Similarly, in planar symmetry, Strickland and Blondin (1995) report a quantitatively different response of the shell for different Mach numbers. While we do not present here any results in that direction and further investigations are certainly needed, we ascribe this behavior to direct or indirect temperature dependences of the growth-rates of many unstable modes. Also, at lower temperatures, the system becomes more stiff and the interaction zone geometrically thinner, requiring a finer numerical grid to capture the essential modes. This point was already pointed out by García-Segura and Mac Low (1995). We are convinced that our high spatial resolution is sufficient to correctly capture the unstable evolution of our model problem.

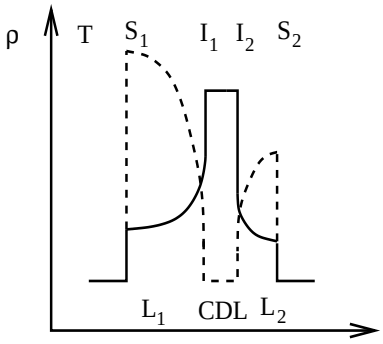

Figure 1. Sketch of the quasi-stationary structure of the interaction zone of radiative colliding flows in density (solid) and temperature (dashed). Note that the main shocks S_1 and S_2 (where the larger part of the bulk energy of the hypersonic free flows is dissipated) as well as the cooling layers L_1, L_2 are stationary with respect to the slowly expanding interfaces I_1, I_2. These interfaces confine the CDL, the thin dense shell of already cooled gas. Also note that within this paper we only look at cases which are symmetric with respect to indices 1,2.

2. Supersonic turbulence in shock compressed thin shells

In this Section we present some results on the supersonic turbulence of the cold part of the interaction zone of hypersonically colliding flows. For this purpose, we define a model problem in Paragraph 2.1. In Paragraph 2.2 we give a brief heuristic description of the supersonic turbulence eventually governing the interaction zone. In Paragraph 2.3 we present some statistical properties of the turbulence. Finally, we give a brief summary in Paragraph 2.4. All simulations presented below were computed with AMRCART, a code combining adaptive meshes with a high resolution finite volume integrator[1].

2.1. Model problem, initial, and boundary conditions

We consider the collision of two flows – parallel and anti-parallel to the x-axis – whose momentum fluxes are balanced (ρ_l = 14 cm^{-3}, v_l = 176 km/s, and ρ_r = 14 cm^{-3}, v_r = -176 km/s). The temperature in both flows is set to 8000 K. We use a two-dimensional domain of 10^{19}cm $\times$ 10^{17}cm with planar geometry. The boundary conditions in y-direction are periodic, in x-direction we use inflow conditions.

To describe the flow, we use 2D Euler equations with a modified energy equation, $\partial E/\partial t + \vec{\nabla}\left[\vec{v}(E+P)\right] = -const \cdot \rho^2\Lambda + H$. The radiative loss function Λ describes optically thin radiative cooling in parameterized form (for details see Cook et al., 1989). Since, to first order, our results do not depend on the exact energy balance, no detailed atomic processes nor explicit ionization/recombination are considered. We further assume that the heating H balances cooling below 8000 K, such that always $T \geq 8000$ K. We use the viscosity associated with our

[1] AMRCART is part of the A-MAZE code package (Walder and Folini, 2000). It is available from http://www.astro.phys.ethz.ch/staff/walder/ or .../folini/.

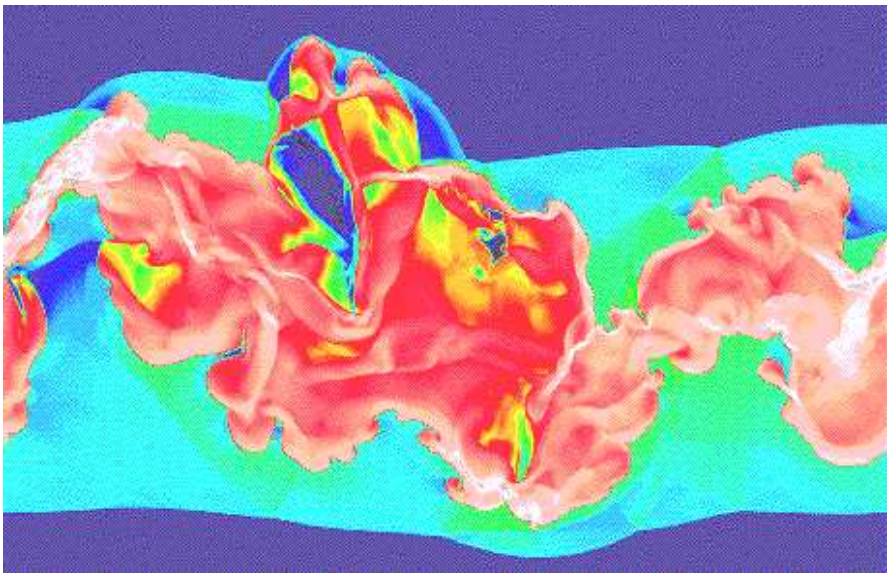

Figure 2. Computed fully developed turbulent interaction zone of run A shown in density. Low density (14 cm^{-3}) is dark, high density is white ($2 \cdot 10^4$ cm^{-3}). The free flows are from the bottom and the top of the graph (x-direction). The main shocks S_1 and S_2 are mostly straight with the exception of a bow shock on the top. The interfaces I_1 and I_2 confining the CDL are visible downstream of the nearly uniform (in density) cooling layers L_1 and L_2. The supersonic turbulence in the CDL forms high-density filaments and knots, next to voids.

numerical method to account for viscous dissipation. Grid studies show that the results are qualitatively similar on differently spaced grids. These physical simplifications – together with the adaptive mesh – allow us to increase the spatial and temporal resolution of our simulation to a degree never reached so far. The finest mesh size is $7.8125 \cdot 10^{13}$ cm squared, resulting in 1280 cells covering the y-range. One time step on the finest level of the mesh was about 0.14 y. One run took 3000 hours of CPU on a CRAY SV1 and 250MB of main memory.

In run A, an initially $1.56 \cdot 10^{15}$ cm thick layer of 8000 K cold gas at rest is placed between the two flows. The layer is in pressure balance with the two free flows and is wiggled with a superposition of different modes. It was integrated till 8200 years. In run B no cold layer is present initially and the interface separating the two free flows is straight. This run was integrated till 5200 years. In both runs the shocks S_i are overstable due to the radiative cooling instability. Note that this instability is responsible for the non-homogeneous formation of the CDL (run B) or introduces large disturbances into the CDL (run A) (Strickland and Blondin, 1995; Walder and Folini, 1996; Walder and Folini, 1998b).

2.2. Heuristic description

Figure 1 shows the very simple, quasi-stationary structure of the collision zone. The flows shock at S_1 and S_2, the shocked gas cools in the layers L_i due to optically thin radiative processes, the cooled gas is compressed into a thin shell (CDL below) by the ram pressure of the hypersonic flows. The steady state post shock temperature is $7 \cdot 10^5$ K, the quasi-stationary density of the CDL is 6567 cm^{-3}. The size of the CDL grows on a time-scale much larger than other dynamical times. Typical cooling times are between 300 ($7 \cdot 10^5$ K) and 900 years ($1.1 \cdot 10^6$ K). Although these parameters are typical for an ionized, circumstellar medium, our results qualitatively carry over to other environments.

Figure 2 shows the computed, turbulent structure. Although only a snapshot, it reflects many features present in the turbulent interaction zone. The shocks into which the undisturbed flows are running may be more or less straight, firmly enclosing the heavily structured cold matter. Or a shock changes into a bow shock, as the cold compressed matter pushes outwards. The shape of the CDL is highly variable, including large scale bending, but with no dominant mode. Momentarily narrow parts of the CDL may spread out a short moment later and vice versa. No particular breathing mode is dominating. The CDL may be singly connected or may enclose large regions of hot gas. The density fluctuates within a large range. We find voids in the neighborhood of highly compressed knots and filaments, reaching values an order of magnitude higher than the quasi-stationary value. The velocity fluctuations are also considerable, reaching from quiet, very subsonic spots to areas in which the flow is highly supersonic. Shocks are present in the CDL, ranging from weak shocklets to strong shocks.

This phenomenology indicates that the interaction zone of the CDL is in a state of supersonic turbulence, and the patchy appearance of the CDL is reminiscent of coherent structures.

2.3. Statistical properties

2.3.1. *Density and its fluctuations*

In supersonic turbulence, density fluctuations are as important as velocity fluctuations. Moreover, they accompany each other, as part of the energy is dissipated in shocks rather than in a vortex cascade. We note already here the significant differences between run A and B, which we will further discuss in Paragraph 2.4.

Firstly, the mean density (Figure 4, left) is far beyond the density of the quasi-stationary structure (= 6567 cm^{-3}). The turbulent pressure balances a significant part of the ram-pressure of the free flows. Figure 4, middle, indicates that most of the mass is concentrated in

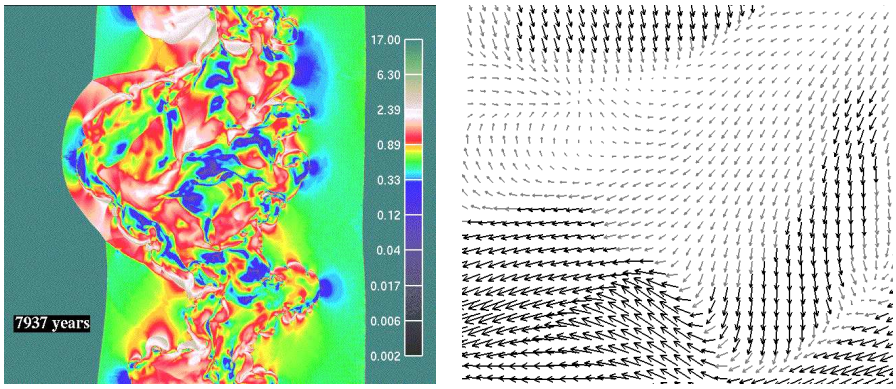

Figure 3. **Left**: Mach numbers in grey scale according to the label at the right side of the graph. The free flows are from the left and the right. **Left**: Velocity field at a particular time in a small range of the CDL. Black arrows show supersonic, grey arrows subsonic flows. Typically, the flow consists of directed patches connected by vorticity dominated areas. Both plots are taken in the rest frame of run A.

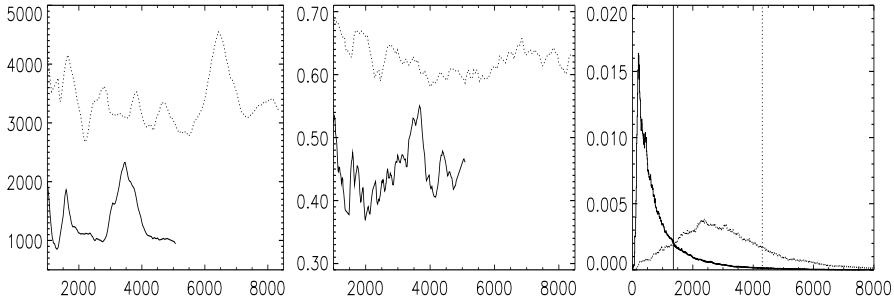

Figure 4. **Left:** Mean density (with respect to volume) of the CDL as a function of time (years). The density of the quasi-stationary pattern is 6567 cm^{-3}. **Middle:** Percentage of mass contained in 80% of the total volume of the CDL as a function of time (years). **Right:** Relative volume as a function of density. The vertical lines denote the masses where, integrating from left to right, 80% of the total volume are reached. (run A, dotted; run B, solid)

a small (run A) or a very small volume (run B). An example (latest time of the two different runs) of the density distribution is given in Figure 4, right. Voids fill most of the volume in run B, regions of small density in run A. However, it is also found that 0.3 percent of the volume in run A and even 4.5 percent of the volume in run B have overcompressed density (i.e. $\rho > 6567\ \mathrm{cm}^{-3}$). Peak densities reach up to 10 times the stationary value. As can be taken from Figure 2 the distribution of these high density regions between the voids is neither an ensemble of many high-density spikes nor is it in the form of one

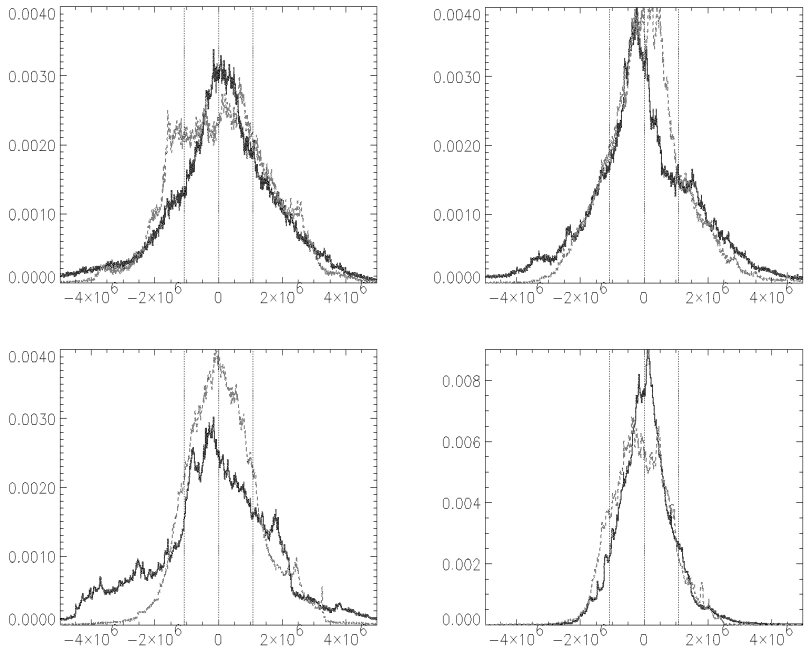

Figure 5. Velocity (in cm/s) distribution (with respect to total volume) of the CDL at different times (upper left T=1768 y, upper right T=3048 y, lower left T=4343 y) for run B and at at time T=5714 y of run A (lower right). x-components are plotted by a solid, y-components by a dashed line. Note the different scale of the y-axis between run A and B.

single high-density area. Rather, a couple of high-density filaments are present, with lengths on the order of the mean width of the CDL and with a ratio of length to widths of several tens. In addition, there are also some more point like high density knots.

2.3.2. *Velocity and its fluctuations*

We first note that the velocity structure isotropizes very rapidly on a large scale: the means for each spatial component scatter around zero. On smaller scales, however, the velocity field can be very anisotropic (see Figure 3, right). The velocity (x- and y-components) distribution of the entire CDL changes very rapidly (see Figure 5). Extremes are a very narrow 'peak'- and an broad 'square'-distribution.

A significant amount of the flow within the CDL is supersonic. Also the velocity field shows a patchy structure, clearly visible in Figure 3. In many patches — and not only in supersonic ones — the flow is nearly uniformly directed. Such patches are partly connected by shocks

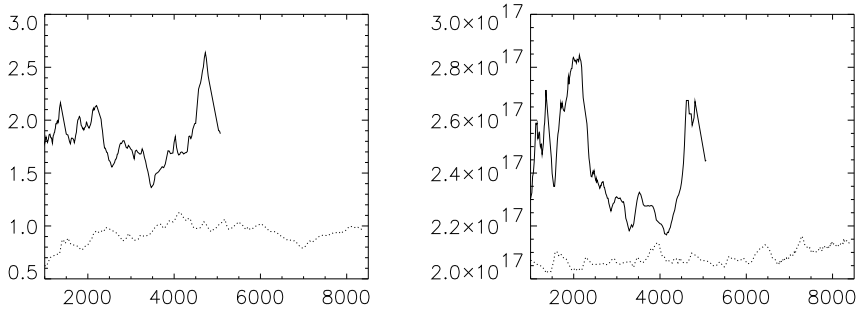

Figure 6. Mean Mach number of CDL (left) and total shock length in cm (right) as a function of time (years) for runs A (dotted) and B (solid). The means are taken with respect to the volume. The sound speed is $1.05 \cdot 10^6$ cm/s.

but also by areas where the flow is strongly vorticity dominated. The patches in density and velocity do not necessarily coincide. We notice, however, that the generally larger mean Mach number in run B (compared to run A) is accompanied by a generally greater total shock length (Figure 6, right). This can be understood since longer shocks are an indication for the existence of bow-shocks and bow shocks destroy less momentum flux than shocks perpendicular to the free flows.

2.4. Summary

We summarize the two most striking results.

1) While the two runs have the same free flow parameters they show very different mean values of important quantities in the interaction zone. Also, run B is in a much more 'violent' regime than run A. This is demonstrated by the much higher mean Mach number and the larger shock length. The more violent character is also immediately apparent when looking at a video animation of the simulation. In a deterministic picture, this can be a consequence of the different initial conditions only. However, in particular the formation process of the CDL and the forcing of the turbulence presumably have a chaotic component, and may, therefore, be co-determining the regime in which the shell actually is, a more smooth or a more violent one. In a statistical sense, they may be as important as the initial conditions.

2) The flow within the turbulent interaction zone has a patchy appearance, nearly no matter in what variable it is displayed. These patches survive for a considerable amount of time. One may consider them to be coherent structures of the turbulence. In density, the patches appear as high-density filaments and voids, in Mach number, as super-

and subsonic areas, and in velocity as areas in each of which the flow particles move in one particular direction. There seems to be no obvious correlation between these different kinds of patches but this point certainly needs a more thorough analysis.

3. Conclusions

Our results show that supersonic turbulence governs the interaction zone of colliding radiative hypersonic flows. The turbulence affects the shape and size of the interaction zone as well as its small scale structure. The interior structure is characterized by highly compressed filaments and knots, large voids, velocities with a supersonic mean and large dispersion, and a cascade of energy dissipating shocks.

Of course, a variety of other physical processes like magnetic fields and radiative forces will be present in different astronomical objects. Our results are also limited by the restriction to 2D. However, analytical considerations and the comparison with simulations of compressible turbulence in a periodic box (Vazquez-Semadeni et al., 1996, Stone et al., 1998, Mac Low, 1999) show that the presented results mirror to a high degree the physical state of colliding flow interaction zones.

For astrophysical objects where colliding radiative flows are present, the turbulence has consequences. Observational quantities and derived variables will be affected; e. g. spectral lines are broader than thermal broadening, and density estimates may be incorrect. Dust formation in some WR-binaries may be favored (e.g. Folini and Walder, 2000b) and the overcompressed regions may trigger star formation in molecular clouds (e.g. Hunter et al., 1986, Klein and Woods, 1998). In connection with cooling flows, overcompression may favor the formation of globular clusters or galaxies. For these objects and for colliding radiative flows in general, these first high resolution computations allow new insights into the physical conditions, including supersonic turbulence.

Acknowledgements

We thank Jean Favre for developing fast multi-block graphics for our adaptive grid data (Favre, 1999) and the referee for fruitful comments.

References

Blondin, J. M. and B. S. Marks: 1996, 'Evolution of cold shock-bounded slabs'. *New Astronomy* **1**, 235–244.

Cook, J. W., C. C. Cheng, V. L. Jacobs, and S. K. Antiochos: 1989, 'Effect of coronal elemental abundances on the radiative cooling'. *The Astrophysical Journal* **338**, 1176–1183.

Draine, B. T. and C. F. McKee: 1993, 'Theory of interstellar shocks'. *ARA&A* **31**, 373–432.

Favre, J.: 1999, 'Accelerating the AVS/Express multi-block visualization macros'. In: *Late Breaking Hot Topics Proceedings of the IEEE Visualization 1999 conference.* in press, http://www.cscs.ch/Official/I2A/SciViz/.

Folini, D. and R. Walder: 2000a. *in preparation.*

Folini, D. and R. Walder: 2000b, 'Theory of thermal and ionization effects in colliding winds of WR+0 binaries'. In: H. J. G. L. M. Lamers and A. Sapar (eds.): *Thermal and Ionization Aspects of Flows from Hot Stars.* pp. 267–278.

García-Segura, G. and M.-M. Mac Low: 1995, 'Wolf-Rayet Bubbles. II. Gasdynamical simulations'. *The Astrophysical Journal* **455**, 160–174.

Grun, J., J. Stamper, C. Manka, J. Resnick, R. Burris, J. Crawford, and B. H. Ripin: 1991, 'Instabilty of Taylor-Sedov blast waves propagating through a uniform gas'. *Phys. Rev. Letters* **66**(21), 2738–2741.

Hunter, H. H., M. T. Sanford, R. S. Whitaker, and R. I. Klein: 1986, 'Star formation in colliding gas flows'. *The Astrophysical Journal* **305**, 309–332.

Klein, R. I. and D. T. Woods: 1998, 'Bending mode instabilities and fragmentation in interstellar cloud collisions: A mechanism for complex structure'. *The Astrophysical Journal* **497**, 777–799.

Mac Low, M. M.: 1999, 'The energy dissipation rate of supersonic, magnetohydrodynamic turbulence in molecular clouds'. *The Astrophysical Journal* **524**, 169–178.

Myasnikov, A. V., S. A. Zhekov, and N. A. Belov: 1998, 'Radiative steady-state colliding stellar wind models: are they correct?'. *Monthly Notices of the Royal Astronomical Society* **298**, 1021–1029.

Stevens, I. R., J. M. Blondin, and A. M. T. Pollock: 1992, 'Colliding winds from early–type stars in binary systems'. *The Astrophysical Journal* **386**, 265–287.

Stone, J. M., E. C. Ostriker, and C. F. Gammie: 1998, 'Dissipation in compressible magnetohydrodynamic turbulence'. *The Astrophysical Journal Letters* **508**, L99–L102.

Strickland, R. and J. M. Blondin: 1995, 'Numerical analysis of the dynamic stability of radiative shocks'. *The Astrophysical Journal* **449**, 727–738.

Vazquez-Semadeni, E., T. Passot, and A. Pouquet: 1996, 'Influence of cooling-induced compressibility on the structure of turbulent flows and gravitational collapse'. *The Astrophysical Journal* **473**, 881–893.

Vishniac, E. T.: 1994, 'Nonlinear instabilites in shock-bounded slabs'. *The Astrophysical Journal* **428**, 186–208.

Walder, R. and D. Folini: 1996, 'Radiative cooling instabilitiy in 1D colliding flows'. *Astronomy and Astrophysics* **315**, 265–284.

Walder, R. and D. Folini: 1998a, 'The formation of knots and filaments in shocks'. *Astrophysics and Space Science* **260**, 215–224. Proc. of the workshop on Hypersonic Radiative Outflows out of Thermal Equilibrium.

Walder, R. and D. Folini: 1998b, 'Knots, filaments, and turbulence in radiative shocks'. *Astronomy and Astrophysics* **330**, L21–L24.

Walder, R. and D. Folini: 2000, 'A-MAZE: A code package to compute 3D magnetic flows, 3D NLTE radiative transfer, and synthetic spectra'. In: H. J. G. L. M. Lamers and A. Sapar (eds.): *Thermal and Ionization Aspects of Flows from Hot Stars: Observations and Theory.* pp. 281–284.